BRAIN
ORIGINAL ARTICLE

Anterior dorsal attention network tau drives visual attention deficits in posterior cortical atrophy

Yuta Katsumi,[1,2,†] Deepti Putcha,[1,3,†] Ryan Eckbo,[1] Bonnie Wong,[1,3] Megan Quimby,[1] Scott McGinnis,[1,2] Alexandra Touroutoglou[1,2,‡] and Bradford C. Dickerson[1,2,3,4,5,‡]

[†,‡]These authors contributed equally to this work.

Posterior cortical atrophy (PCA), usually an atypical clinical syndrome of Alzheimer's disease, has well-characterized patterns of cortical atrophy and tau deposition that are distinct from typical amnestic presentations of Alzheimer's disease. However, the mechanisms underlying the cortical spread of tau in PCA remain unclear. Here, in a sample of 17 biomarker-confirmed (A+/T+/N+) individuals with PCA, we sought to identify functional networks with heightened vulnerability to tau pathology by examining the cortical distribution of elevated tau as measured by ^{18}F-flortaucipir (FTP) PET. We then assessed the relationship between network-specific FTP uptake and visuospatial cognitive task performance. As predicted, we found consistent and prominent localization of tau pathology in the dorsal attention network and visual network of the cerebral cortex. Elevated FTP uptake within the dorsal attention network (particularly the ratio of FTP uptake between the anterior and posterior nodes) was associated with poorer visuospatial attention in PCA; associations were also identified in other functional networks, although to a weaker degree. Furthermore, using functional MRI data collected from each patient at wakeful rest, we found that a greater anterior-to-posterior ratio in FTP uptake was associated with stronger intrinsic functional connectivity between anterior and posterior nodes of the dorsal attention network. Taken together, we conclude that our cross-sectional marker of anterior-to-posterior FTP ratio could indicate tau propagation from posterior to anterior dorsal attention network nodes, and that this anterior progression occurs in relation to intrinsic functional connectivity within this network critical for visuospatial attention. Our findings help to clarify the spatiotemporal pattern of tau propagation in relation to visuospatial cognitive decline and highlight the key role of the dorsal attention network in the disease progression of PCA.

1 Frontotemporal Disorders Unit, Massachusetts General Hospital and Harvard Medical School, Boston, MA 02114, USA
2 Department of Neurology, Massachusetts General Hospital and Harvard Medical School, Boston, MA 02114, USA
3 Department of Psychiatry, Massachusetts General Hospital and Harvard Medical School, Boston, MA 02114, USA
4 Alzheimer's Disease Research Center, Massachusetts General Hospital and Harvard Medical School, Boston, MA 02114, USA
5 Athinoula A. Martinos Center for Biomedical Imaging, Massachusetts General Hospital and Harvard Medical School, Boston, MA 02114, USA

Correspondence to: Dr Yuta Katsumi
149 13th St, Charlestown
MA 02129, USA
E-mail: ykatsumi@mgh.harvard.edu

Received February 10, 2022. Revised May 16, 2022. Accepted June 21, 2022. Advance access publication October 14, 2022

Correspondence may also be addressed to: Dr Deepti Putcha
E-mail: dputcha@mgh.harvard.edu

Keywords: hyperphosphorylated tau; positron emission tomography; Alzheimer's disease; functional networks; functional connectivity

Abbreviations: Aβ = amyloid-β; DAN = dorsal attention network; FEF = frontal eye fields; FTP = ^{18}F-flortaucipir; PCA = posterior cortical atrophy; PiB = ^{11}C-Pittsburgh compound B; SUVR = standardized uptake value ratio; VOSP = Visual Object Space Processing battery

Introduction

Posterior cortical atrophy (PCA) syndrome is defined clinically by a progressive decline in higher-order visuospatial and visuoperceptual processing, often with elements of Gerstmann syndrome with relative preservation in other cognitive domains, and is associated with atrophy and hypometabolism in posterior parietal, temporal and/or occipital cortical regions.[1–5] PCA is most commonly, but not always, associated with Alzheimer's disease neuropathological changes [ADNC; including amyloid-β (Aβ) plaques, hyperphosphorylated tau neurofibrillary tangles, tau-immunoreactive dystrophic neurites, neuronal loss and gliosis, etc.].[6,7] It has been referred to as the visual variant of Alzheimer's disease,[8] and the localization of ADNC is more prominent in posterior cortical regions than in cases of typical amnestic Alzheimer's disease dementia.[9,10] Consistent with the clinical symptoms of PCA, previous tau PET studies have identified *in vivo* evidence of neurodegeneration (atrophy or hypometabolism) that is co-localized with tau pathology most prominently in these posterior cortical regions.[11–16] Although the unique spatial pattern of tau deposition has been characterized in PCA, the mechanisms underlying the cortical spread of tau in this syndrome remain relatively unclear. Capitalizing on large and heterogeneous samples, a recent tau PET study revealed four distinct spatiotemporal patterns of cortical tau distribution across the syndromic spectrum of Alzheimer's disease.[17] One of these trajectories was characterized by early tau deposition in the occipital and posterior temporoparietal cortices with gradual anterior progression, although the link between this pattern of tau spread and the salient clinical symptoms of PCA has not been formally established. In the present study, we addressed this gap in the literature by examining possible network-based mechanisms underlying tau propagation and its relation to visual cognitive symptoms in PCA.

Emerging multimodal neuroimaging evidence supports the hypothesis that pathological tau proteins spread through neuronal networks in human cerebral cortex.[18] Multiple recent studies have focused on the link between tau accumulation and functional connectivity and have demonstrated that pairs of cortical regions with stronger intrinsic functional connectivity in the healthy brain exhibit higher covariance in tau accumulation in patients across the syndromic spectrum of symptomatic Alzheimer's disease.[19–21] Cortical regions showing stronger functional connectivity with high-tau regions (tau 'hot spots') also show high levels of tau accumulation.[19] Furthermore, the magnitude of intrinsic functional connectivity is a stronger predictor of longitudinal cortical tau spread than the proximity (Euclidian distance) of the connected regions in Alzheimer's disease.[22]

PCA is associated with disruption of several large-scale functional networks in the cerebral cortex, and the spatial topography of these networks overlaps with the localization pattern of tau in this clinical syndrome. Specifically, the visual network as well as the posterior regions of the dorsal attention (e.g. superior parietal lobule) and default (e.g. posterior cingulate cortex) networks have been reported as showing hypometabolism,[23–26] atrophy,[14,15,25,27] and structural and functional hypoconnectivity.[27–31] The dorsal attention network (DAN), comprising key nodes including the superior parietal cortex, posterior middle temporal gyrus (area MT; MT+) and the caudal middle frontal gyrus (frontal eye fields; FEF),[32,33] may be particularly important for PCA because of its critical role in visuospatial attention.

Although much of the prior research on PCA emphasizes the involvement of posterior cortical regions in this syndrome, additional evidence points toward dysfunction of the FEF, the core anterior node of the DAN. Prior reports describe FEF hypometabolism,[23,26] hypoperfusion,[34] and atrophy[35] in PCA. Hypometabolism in the FEF in PCA has been interpreted as occurring secondary to degeneration of the afferent input from occipitotemporal regions involved in visual processing and is thought to be the cause of oculomotor apraxia (impaired voluntary control of eye movements) in PCA.[26] Neurodegeneration in PCA is first observed in posterior cortical regions. As the disease progresses, neurodegeneration is then observed in anterior cortical regions. Given that local tau accumulation is thought to precede neurodegeneration in Alzheimer's disease,[36] the accumulation of tau also likely happens first in the posterior cortical regions, followed by accumulation in the more anterior regions. This is consistent with recent longitudinal evidence showing that PCA patients, who already had elevated tau in the occipital and posterior temporo-parietal areas, exhibited the highest annual rates of tau accumulation in the lateral frontal cortices.[37] The degree of longitudinal tau accumulation was recently shown to be directly associated with the magnitude of intrinsic functional connectivity in PCA at the level of the whole cerebral cortex.[21] Collectively, these findings provide support to the hypothesis that propagation of tau pathology from the posterior to the anterior cortical regions in PCA may be facilitated by functional connectivity within the DAN, a network that plays a key role in the clinico-pathophysiology of PCA. That is, tau deposition begins in the posterior parietal and occipitotemporal regions and over time propagates anteriorly to the FEF, accompanied by progressive decline in visual attention. However, to our knowledge, no published study has examined the potential mechanisms of tau spread within specific brain networks relevant to the clinical symptomatology of PCA.

The goal of the current study was to identify functional networks with heightened vulnerability to tau pathology in PCA by examining the cortical distribution of elevated tau pathology as measured by ^{18}F-flortaucipir (FTP) PET within the context of a mapping of networks in the healthy brain.[38] We hypothesized that (i)

the majority of our PCA patients would exhibit FTP evidence of tau pathology in the visual network and posterior nodes of the DAN of the brain, consistent with visuospatial and visuoperceptual impairment that is characteristic of this syndrome. We further hypothesized that (ii) greater tau pathology within these functional networks would be associated with poorer visuospatial cognitive task performance across patients. In light of the recent evidence discussed above highlighting the dysfunction of the frontal nodes (FEF) of the DAN in PCA, we also investigated regional variability in FTP uptake within this network (i.e. anterior versus posterior nodes). Specifically, we developed a Tau Network Propagation Index, here computed as the anterior-to-posterior ratio in elevated FTP uptake. This is a putative, cross-sectional index of intranetwork tau spread measured at the individual participant level. We used this Tau Network Propagation Index to test the hypothesis that (iii) individual patients with a greater anterior-to-posterior ratio in FTP uptake in DAN, possibly reflective of spreading of tau within this network, would be more impaired in visuospatial cognitive task performance. Finally, to better understand the link between tau accumulation and intrinsic functional connectivity within the DAN in PCA, we analysed functional MRI data collected at wakeful rest. We hypothesized that, across individual patients, (iv) the greater anterior-to-posterior ratio in FTP uptake (possibly indicative of more advanced tau propagation from the posterior to the anterior nodes) within the DAN would be associated with stronger intrinsic functional connectivity between these nodes of the same network.

Materials and methods

Participants

Seventeen amyloid-, tau-, and neurodegeneration-positive (A+/T+/N+)[39] individuals diagnosed with PCA were included in this study, all of whom were recruited from the Massachusetts General Hospital (MGH) Frontotemporal Disorders Unit PCA program[7,40] (see Table 1 for demographic and clinical data). All patients received a standard clinical evaluation comprising a structured history obtained from both patient and informant, comprehensive neurological and psychiatric history as well as neuropsychological assessment. Clinical formulation was performed through consensus conference by our multidisciplinary team of neurologists, neuropsychologists, and speech and language pathologists, with each patient classified based on all available clinical information as having mild cognitive impairment or dementia (Cognitive Functional Status), cognitive-behavioural syndrome and likely aetiological diagnosis.[6] All patients met diagnostic criteria for PCA[2] and underwent neuroimaging sessions which included structural MRI, resting-state functional MRI, and ^{11}C-Pittsburgh compound B (PiB) and FTP PET scans. Aβ positivity was determined by visual read according to previously published procedures[41] as well as a summary distribution volume ratio (DVR) of frontal, lateral, and retrosplenial (FLR) regions greater than 1.2.[42] We excluded a subset of patients from our analyses due to the lack of visuospatial cognitive data (n = 2, for brain–behaviour correlation analyses) or resting-state functional MRI data (n = 1, for FTP–connectivity correlation analyses) (see below).

Table 1 Clinical characteristics of patients with PCA likely due to Alzheimer's disease

Demographics	PCA (n = 17)
Age, years	68.7 ± 8.3
Sex, male/female	7/10
Education, years	17.0 ± 2.0
MoCA	19.2 ± 5.9
CDR	0.5 (n = 10), 1 (n = 6), 2 (n = 1)
CDR-SOB[a]	6.2 ± 4.8
PiB FLR DVR	1.9 ± 0.3

CDR = Clinical Dementa Rating scale; MoCA = Montreal Cognitive Assessment; PiB FLR DVR = Pittsburgh compound B frontal-lateral-retrosplenial distribution volume ratio; SOB = Sum of Box scores.
[a]Based on n = 16.

We included a group of amyloid-negative (Aβ–) cognitively normal individuals, all of whom performed within normal limits on neuropsychological testing, had normal brain structure based on MRI and low cerebral amyloid based on quantitative analysis of PiB PET data (FLR DVR < 1.2), resulting in a cognitively normal sample of 22 individuals (mean age = 68 ± 4.13, 11 male/11 female). This control sample was used as a reference for quantifying elevated FTP uptake in our patients. Individuals were excluded from our patient and control groups if they had a primary psychiatric or other neurological disorder including major cerebrovascular infarct or stroke, seizure, brain tumour, hydrocephalus, multiple sclerosis, HIV-associated cognitive impairment or acute encephalopathy. This work was carried out in accordance with The Code of Ethics of the World Medical Association (Declaration of Helsinki) for experiments involving humans. All participants and their informants/caregivers provided informed consent in accordance with the protocol approved by the MassGeneral Brigham HealthCare System Human Research Committee Institutional Review Board in Boston, Massachusetts.

Assessment of visuospatial cognition

Within a maximum of 72 days from the PET and MR sessions (mean interval = 15.9 ± 19.8), 15 of the 17 Aβ+ PCA patients underwent a neuropsychological test battery. Our focus in this study was to measure visuospatial attention, a common cognitive deficit characterizing PCA. To do this, we used the Visual Object Space Processing battery (VOSP) Number Location test.[43] In this task, 10 arrays are presented and each array is comprised of two squares arranged one above the other. The top square contains numbers arranged randomly, whereas the bottom square contains only a black dot. The patient is asked to verbally identify which number corresponds to the same spatial location as the black dot. Each correct identification earns one point, thus the possible score ranges from 0 to 10. Participants who could not demonstrate adequate comprehension of task instructions or adequate visual perceptual abilities necessary to engage in this task were excluded from this study. Performance on the VOSP Number Location test has been associated with indices of regional tau deposition and atrophy in PCA.[14,44] Our focus on the VOSP Number Location test was also informed by the observation that this measure had the greatest range in performance of all the tests administered in this study, enabling us to better measure brain–behaviour relationships (Supplementary Table 1).

Neuroimaging data acquisition and preprocessing

All participants underwent FTP and PiB PET scans. The FTP radiotracer was prepared at MGH with a radiochemical yield of 14 ± 3% and specific activity of 216 ± 60 GBq/μmol (5837 ± 1621 mCi/μmol) at the end of synthesis (60 min) and validated for human use.[45]

The PiB radiotracer was prepared as described previously,[46] with minor modifications. All PET data were acquired using a Siemens/CTI (Knoxville, TN) ECAT HR+ scanner: 3D mode, 63 imaging planes, 15.2 cm axial field of view, 5.6 mm transaxial resolution and 2.4 mm slice interval. FTP PET images were acquired from 80 to 100 min after a 10.0 ± 1.0 mCi bolus injection in 4 × 5 min frames. PiB PET images were acquired with an 8.5–10.5 mCi bolus injection followed immediately by a 60 min dynamic acquisition in 69 frames (12 × 15 s, 57 × 60 s). All PET data were reconstructed and attenuation corrected; each frame was evaluated to verify adequate count statistics; interframe head motion was corrected prior to further processing.

MRI data were acquired from each participant using a Siemens Tim Trio 3.0 Tesla scanner, which included a structural MRI scan using a T_1-weighted multi-echo magnetization prepared rapid acquisition sequence [MEMPRAGE; repetition time (TR) = 2530 ms, echo times (TEs) = 1.64/3.5/5.36/7.22 ms, flip angle (FA) = 7°, slice thickness = 1 mm, field of view (FoV) = 256 mm, 0% slice gap) as well as a functional MRI scan at wakeful rest using an echo-planar imaging sequence (TR = 5000 ms, TE = 30 ms, FA = 90°, slice thickness = 2 mm, FoV = 256 mm, 0% slice gap, 76 volumes).

Each participant's MEMPRAGE data underwent intensity normalization, skull stripping, and an automated segmentation of cerebral white matter to locate the grey–white boundary via FreeSurfer v6.0, which is documented and freely available for download online (http://surfer.nmr.mgh.harvard.edu). Defects in the surface topology were corrected[47] and the grey/white boundary was deformed outward using an algorithm designed to obtain an explicit representation of the pial surface. We visually inspected each participant's cortical surface reconstruction for technical accuracy and manually edited it when necessary. Whole-cortex maps of cortical thickness (estimated by the distance between the white and pial surfaces at each vertex) were registered to a template surface space (fsaverage) and smoothed geodesically with full-width-half-maximum (FWHM) of 10 mm.

We performed further processing of FTP PET data via the PetSurfer tools.[48,49] Each participant's FTP PET data were first rigidly co-registered to their anatomical volume and the accuracy of cross-modal spatial registration was confirmed by visual inspection. FTP PET data were then corrected for partial volume effects. Specifically, based on each participant's high-resolution tissue segmentation derived by the standard Desikan–Killiany atlas in FreeSurfer,[50] the symmetric geometric transfer matrix (GTM) method was used to correct for spill-in and spill-out effects between adjacent brain tissue types, with a point spread function of 6 mm.[48,49] Using partial volume-corrected FTP data, we derived the standardized uptake value ratio (SUVR) image per participant with whole cerebellar grey matter as a reference region.[51] SUVR maps were then resampled to fsaverage space and smoothed geodesically with FWHM of 8 mm. PiB PET data were similarly processed via the PetSurfer tools and were used to derive FLR DVR for the confirmation of Aβ positivity.[15] In addition, for each patient, we estimated global cortical Aβ by calculating the mean PiB SUVR (40–60 min) across all cortical vertices.

To identify areas of the cerebral cortex showing elevated FTP uptake, we calculated for each PCA patient a vertex-wise W-score map.[52–54] W-scores are analogous to Z-scores adjusted for specific covariates of no interest, which in this study were age and sex. A detailed description of W-score calculation has been provided elsewhere.[12,55,56] Briefly, we first performed a vertex-wise multiple regression analysis using FTP SUVR data from Aβ− cognitively normal participants, which resulted in whole-cortex beta coefficient maps of age and sex, as well as individual maps of residuals. We then computed W-scores for each patient using the following formula:

$$W = \frac{SUVR_{actual} - SUVR_{predicted}}{SD_{residuals}}$$

where $SUVR_{actual}$ = the observed SUVR of a given patient, $SUVR_{predicted}$ = the predicted SUVR based on age and sex of a given patient as well as beta coefficients obtained from Aβ− cognitively normal participants and $SD_{residuals}$ = the standard deviation of the individual residual maps obtained from Aβ− cognitively normal participants. Following previous studies examining this measure,[53,54] we used a threshold of $W > 1.65$, corresponding to the 95th percentile of a normal distribution, to define abnormal FTP uptake at each vertex in each patient. Using this threshold, we binarized W-score maps from all patients, summed all the maps, and divided by 17. Once converted to a percentage in this way, the resulting W-score 'overlap' map depicts the percentage of individuals in this sample of PCA patients with elevated FTP signal at each vertex point across the entire cortical mantle. Following a similar procedure, we also calculated for each patient W-score maps using cortical thickness data; these maps were used to estimate the degree of cortical atrophy.

Preprocessing of resting-state functional MRI data involved the following steps that have been previously established[57–59] and used in our group.[52,60–64] Removal of the first four volumes to allow for T_1 equilibration, slice timing correction, head motion correction using the first volume as reference, spatial normalization to the MNI152 template, low-pass filtering at 0.08 Hz, and volumetric smoothing with FWHM of 6 mm. We then performed linear regression on the preprocessed data to account for sources of spurious variance, which included raw time series and first-order temporal derivatives of six motion parameters, global signal, mean white matter signal, and mean ventricular CSF signal. The residual time series data from each patient were submitted to group-level statistical analyses described below.

Statistical analysis

Using individual FTP SUVR maps as inputs, we first created a whole-cortex vertex-wise general linear model (GLM) in FreeSurfer to identify areas of the cerebral cortex where PCA patients showed greater FTP uptake than Aβ− cognitively normal participants. For this analysis, statistical significance was assessed with a vertex-wise threshold of $P < 0.0001$. The resulting vertex-wise significance map was converted to a binary mask, within which we examined the magnitude of the mean group difference at each vertex (ΔFTP SUVR). To characterize the spatial topography of abnormal FTP signal in PCA with respect to large-scale functional networks of the cerebral cortex, we utilized an established cerebral cortical parcellation consisting of 400 parcels, each of which belonged to one of the seven canonical networks (i.e. visual, somatomotor, dorsal attention, ventral attention, limbic, frontoparietal, and default).[38,65] Here, we adhere to the original and conventional use of these networks, although we acknowledge that the 'default' and 'limbic' networks are not always distinguished in the literature[66] and that both networks contain agranular, limbic tissue.[67,68] We used the same network parcellation to characterize the topography of spatial overlap in elevated FTP uptake across Aβ+ PCA patients.

To test our hypotheses regarding the relationship between elevated FTP uptake and visual cognitive task performance, we

computed the Pearson's product moment correlation between the mean *W*-scores calculated within our specific a priori networks of interest (i.e. visual network and DAN) and performance on the VOSP Number Location test across patients. To further assess regional variability within the DAN, we subdivided this network into the anterior and posterior components based on the relative location of the parcels in the cerebral cortex. The resulting anterior DAN consisted of parcels corresponding to bilateral FEF and ventral precentral gyrus (10 parcels in total), whereas the posterior DAN included bilateral superior parietal lobule and area MT (36 parcels in total; Supplementary Fig. 1). We then computed a Tau Network Propagation Index within the DAN—a putative, cross-sectional index of tau spread within this network—as the ratio of the mean *W*-scores between the anterior and posterior DAN subnetworks and investigated its association with visual cognitive task performance. Moreover, we performed additional correlation analyses between cortical thickness within each network of interest (also expressed as mean *W*-scores) and VOSP Number Location test performance; these analyses enabled comparisons of the effects of tau and atrophy within the same networks. Although not directly relevant for our *a priori* hypotheses, we also investigated the relationships between FTP uptake in networks other than the visual network and the DAN and VOSP Number Location test performance. Additionally, we tested for the relationships between FTP uptake in the DAN and task performance in cognitive domains other than visuospatial attention (see the Supplementary material). Results of these analyses helped clarify the specificity of the observed effects identified by our main analyses.

Finally, we performed a cross-modal correlation analysis to test our hypothesis about the link between the Tau Network Propagation Index and intrinsic functional connectivity within the DAN across patients. To put FTP PET data into the same analysis space as resting-state functional MRI data, we calculated the mean *W*-score for each parcel part of the DAN according to the Schaefer parcellation.[65] For each unique pair of an anterior and a posterior parcel, we then calculated (i) the Tau Network Propagation Index; and (ii) the *Z*-transformed Pearson's *r*-value obtained from correlating the mean residual time series. These values were calculated for each patient and the Pearson's *r* was computed for each parcel pair across all patients. Given our relatively small sample size and *a priori* hypothesis concerning specific functional networks, statistical significance of all brain–behaviour and tau–connectivity correlations was assessed at $P < 0.05$ uncorrected for multiple comparisons. To ensure that the observed associations between FTP uptake and VOSP Number Location task performance or functional connectivity was not confounded by amyloid load, we additionally computed partial correlations between these variables controlling for global cortical Aβ across patients.

Data availability

The data that support the findings of this study are available from the corresponding authors, upon reasonable request.

Results

Clinical characteristics of biomarker-confirmed PCA patients

Table 1 summarizes the clinical characteristics of the A+/T+/N+ PCA patients in this sample. Patients included in this study were classified as either having mild cognitive impairment [clinical dementia rating (CDR) = 0.5], mild dementia (CDR = 1) or moderate dementia (CDR = 2), with the majority (10/17) rated at the stage of mild cognitive impairment. Supplementary Table 1 includes test performance across cognitive domains. As expected in this sample of A+/T+/N+ PCA patients, the most striking areas of impairment were in the visuospatial domain including in visuospatial attention and working memory, figure copy, and visual confrontation naming. In contrast, auditory naming, auditory attention, and memory recognition discriminability were largely spared.

Functional network characterization of cortical tau deposition in PCA

A whole-cortex vertex-wise GLM revealed that, compared with Aβ– cognitively normal participants, Aβ+ PCA patients exhibited prominent FTP uptake in the occipital, ventral and lateral temporal, lateral and medial parietal, and lateral frontal cortices bilaterally (Fig. 1A). These regions included bilateral FEF, superior parietal lobule, and area MT, which are key nodes of the DAN. To further characterize the spatial topography of cortical tau deposition, we calculated the mean FTP SUVR across all vertices falling within the boundaries of each of the seven canonical functional networks.[38,65] As expected, the largest effect size of between-group differences was observed in the visual network and DAN (Fig. 1B).

Next, we examined the consistency of elevated FTP signal across all patients by computing vertex-wise *W*-scores for each patient. From these *W*-score maps, we generated a group-level *W*-score overlap map, which allowed us to calculate the percentage of patients in this sample with elevated FTP uptake at each cortical vertex. This analysis revealed that, in line with the SUVR results reported above, the visual network and DAN were most consistently affected, with 100% of the patients in this sample showing elevated FTP uptake in at least some parts of these two networks, including a small prefrontal region co-localized with the FEF (Fig. 2).

Elevated FTP uptake in the DAN is associated with impaired visuospatial cognitive task performance

To assess the behavioural significance of elevated FTP uptake in the visual network and DAN, we performed a series of bivariate correlation analyses and examined the relationships between network-wise mean *W*-scores and performance on the VOSP Number Location test across patients. In addition to targeting these two networks as a whole, we also separately investigated elevated FTP uptake in the anterior DAN, the posterior DAN, as well as the ratio between the two. Further, by performing similar correlation analyses using cortical thickness data, we directly compared the effects of tau accumulation and atrophy within the same networks and their relations to visuospatial cognitive function.

At the overall network level, elevated FTP uptake in the DAN, but not the visual network, was associated with worse performance on the VOSP Number Location test at a conventional threshold of $P < 0.05$ (Fig. 3). Our examination of anterior versus posterior components of the DAN revealed that this negative relationship was specifically driven by its anterior subnetwork. Furthermore, of all the network variables, the anterior-to-posterior ratio in FTP uptake (our Tau Network Propagation Index) was the strongest correlate of visuospatial cognitive impairment. Analyses of partial correlations among these variables controlling for global cortical Aβ yielded overall similar results; elevated FTP uptake in the anterior DAN ($r = -0.68$, $P \leq 0.008$) but not posterior DAN ($r = -0.27$, $P \leq 0.36$) was associated with poorer performance on the VOSP Number

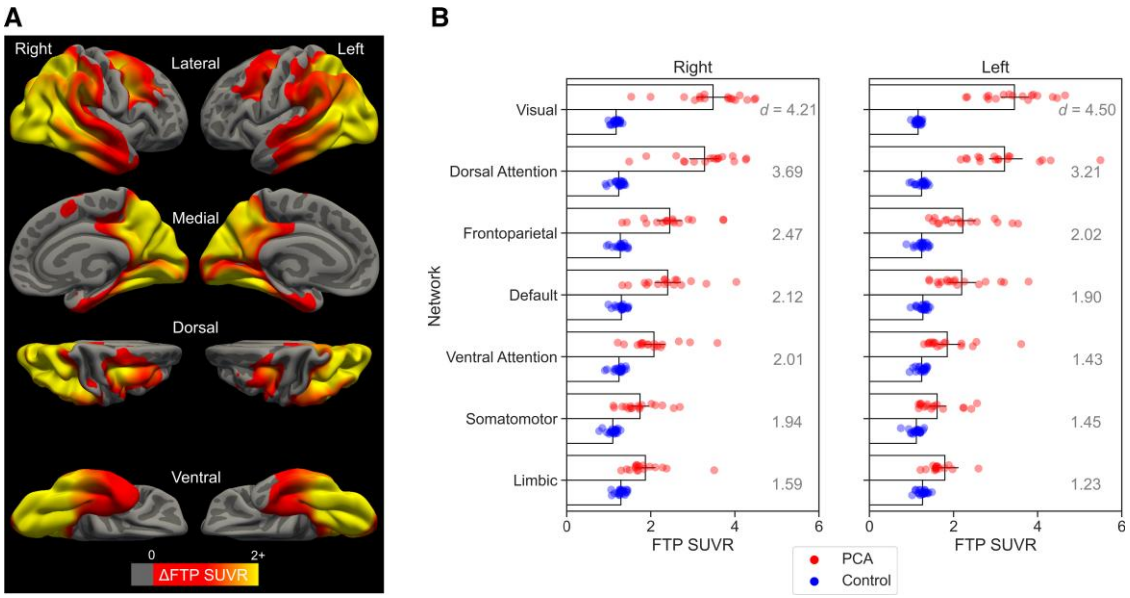

Figure 1 Group comparison of FTP uptake between patients with PCA likely due to Alzheimer's disease ($n = 17$) versus Aβ− cognitively normal participants ($n = 22$). (**A**) Coloured vertices on the cortical surface map indicate areas where PCA patients had greater FTP SUVR then controls. (**B**) Bar plots represent the mean FTP SUVR values calculated for each of the seven canonical functional networks separately for each group. The networks are roughly ordered, from *top* to *bottom*, by the effect size (Cohen's *d*) of between-group differences. All between-group comparisons are significant at $P < 0.001$. Coloured circles overlaid on the bar plot represent individual participants in each group.

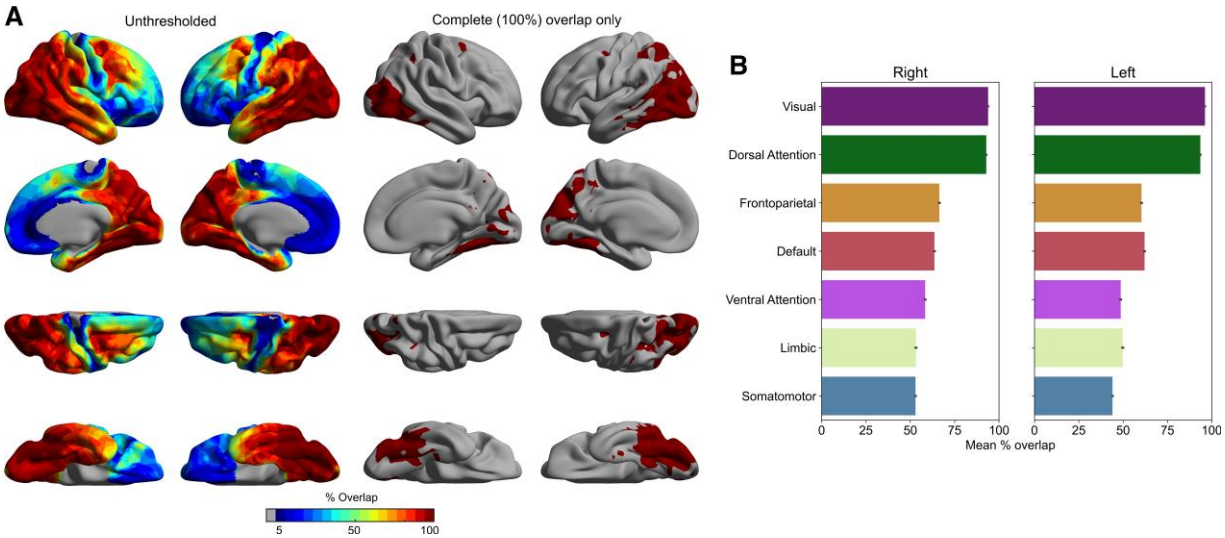

Figure 2 Between-patients consistency in the cortical distribution of elevated FTP uptake in PCA. (**A**) Coloured vertices on the cortical surface map indicate the percentage of PCA patients in this sample with elevated FTP uptake ($n = 17$). All patients exhibited elevated FTP uptake in the occipitotemporal (including area MT) and occipitoparietal (including superior parietal lobule) cortices, as expected, as well as a small prefrontal region co-localized with the FEF, bilaterally. (**B**) Bar plots represent the mean between-patients overlap calculated for each of the seven canonical functional networks.[38] Across all patients, elevated FTP uptake was most consistently observed within the visual network and DAN. Error bars denote 1 standard error of the mean.

Location test, with the Tau Network Propagation Index being the strongest correlate ($r = -0.77$, $P \leq 0.001$). Comparisons of network-wise mean W-scores revealed that, on average, FTP uptake was most elevated in the visual network (mean = 16.68, SD = 5.19) followed by the posterior DAN (mean = 11.69, *SD* = 4.31) then by the anterior DAN (mean = 6.94, SD = 3.86); visual versus posterior DAN: $t = 6.71$, $P \leq 0.001$, $d = 1.63$; posterior DAN versus anterior DAN: $t = 6.71$, $P \leq 0.001$, $d = 1.63$; visual versus anterior DAN: $t = 10.00$, $P \leq 0.001$, $d = 2.43$.

Greater cortical thickness in the visual network and DAN was associated with better visuospatial cognitive task performance (Fig. 3). Examination of the DAN subnetworks revealed that the observed relationship between cortical thickness and task performance was specifically driven by the posterior DAN. The

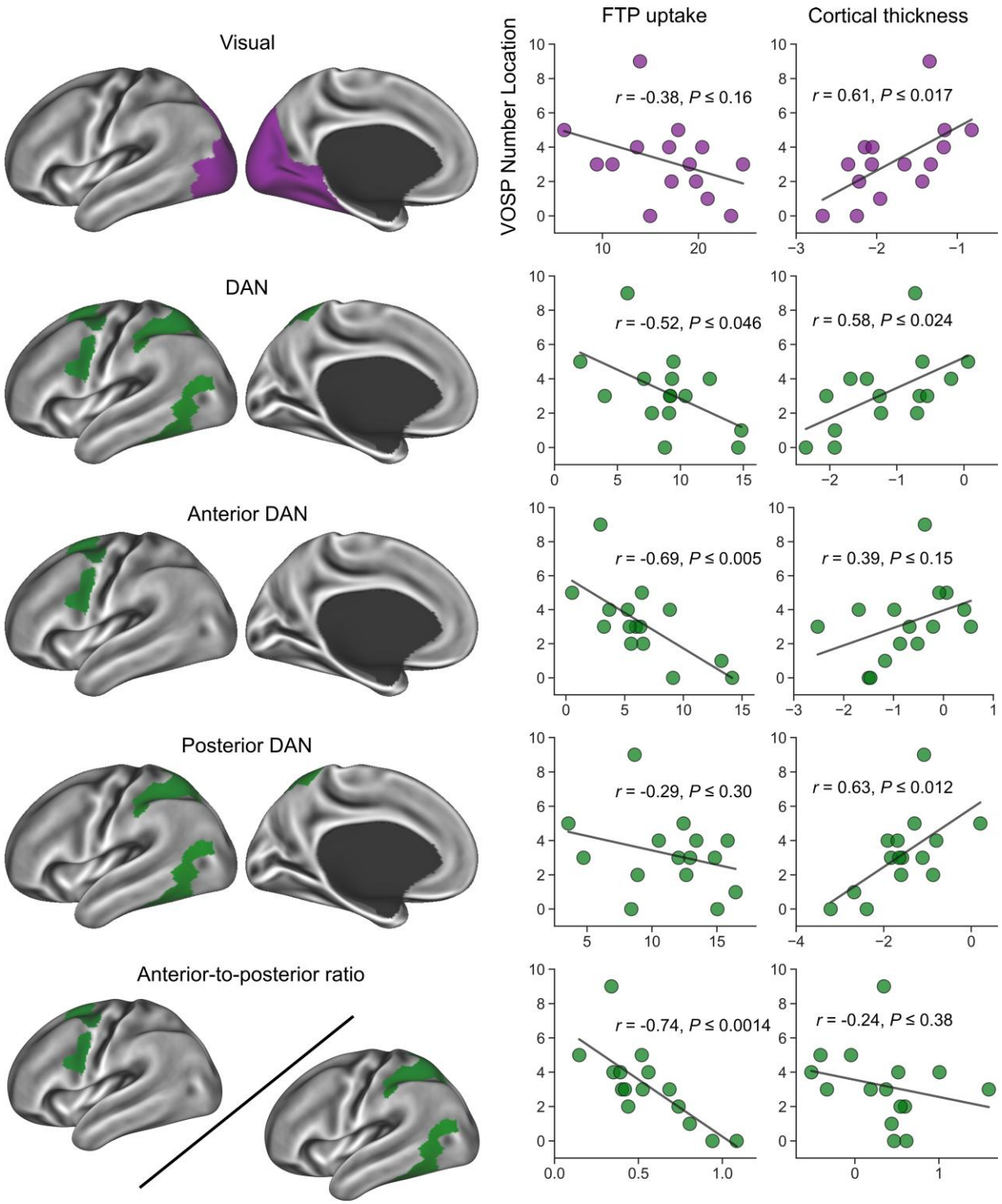

Figure 3 Elevated FTP uptake in the anterior DAN is associated with impaired performance in the VOSP number location test. Coloured vertices on the cortical surface maps indicate the areas from which FTP signal (mean W-scores) was extracted for each patient and correlated with VOSP number location test performance. VOSP performance was not related to FTP signal within the visual network, but had a negative correlation within the DAN. When the DAN was split into its subnetworks, VOSP performance was found to be strongly negatively correlated with elevated FTP signal in the anterior DAN, but not the posterior DAN. VOSP performance showed the most robust negative correlation with the anterior-to-posterior DAN FTP signal ratio (the Tau Network Propagation Index).

anterior-to-posterior ratio in cortical thickness calculated analogously to the Tau Network Propagation Index was not associated with visual cognitive task performance. On average, the anterior DAN was less atrophic (mean = –0.82, SD = 0.83) than the posterior DAN (mean = –1.67, SD = 0.83) or visual network (mean = –1.84, SD = 0.55), with the latter two showing comparable cortical thickness; anterior DAN versus posterior DAN: $t = 4.65$, $P \leq 0.001$, $d = 1.13$; anterior DAN versus visual: $t = 5.57$, $P \leq 0.001$,

$d = 1.35$; posterior DAN versus visual: $t = 1.41$, $P \leq 0.177$, $d = 0.34$. Importantly, the relationship between elevated FTP uptake in the anterior DAN and visuospatial cognitive task performance remained significant after controlling for cortical thickness in the same subnetwork ($r = -0.64$, $P \leq 0.014$); similarly, the degree of correlation between the Tau Network Propagation Index and task performance did not change fundamentally when the ratio of thickness between the anterior and posterior DAN was controlled for ($r = -0.74$, $P \leq 0.003$).

Stronger DAN connectivity is associated with an index of greater intranetwork tau spread

Finally, we evaluated the possible link between the spread of tau and neuronal communication within the DAN by examining the magnitude of correlations between the Tau Network Propagation Index among all unique pairs of the anterior–posterior parcels and intrinsic functional connectivity between the corresponding parcels. This analysis demonstrated that stronger intrinsic functional connectivity between the anterior and posterior DAN was associated with a greater ratio in FTP uptake between the corresponding parcels (Fig. 4). Significant correlations were exclusively identified between the parcels anatomically corresponding to the FEF (anterior) and the superior parietal lobule (posterior). All suprathreshold correlations between the Tau Network Propagation Index and intrinsic functional connectivity remained significant and largely unchanged after controlling for global cortical Aβ in each patient (Supplementary Fig. 2).

Discussion

Recent studies utilizing large-scale and heterogeneous data sets have yielded emerging evidence for unique spatiotemporal patterns of cortical tau spread across the full symptomatic and syndromic spectrum of Alzheimer's disease.[17,22,69,70] Although such evidence is useful in systematically characterizing the

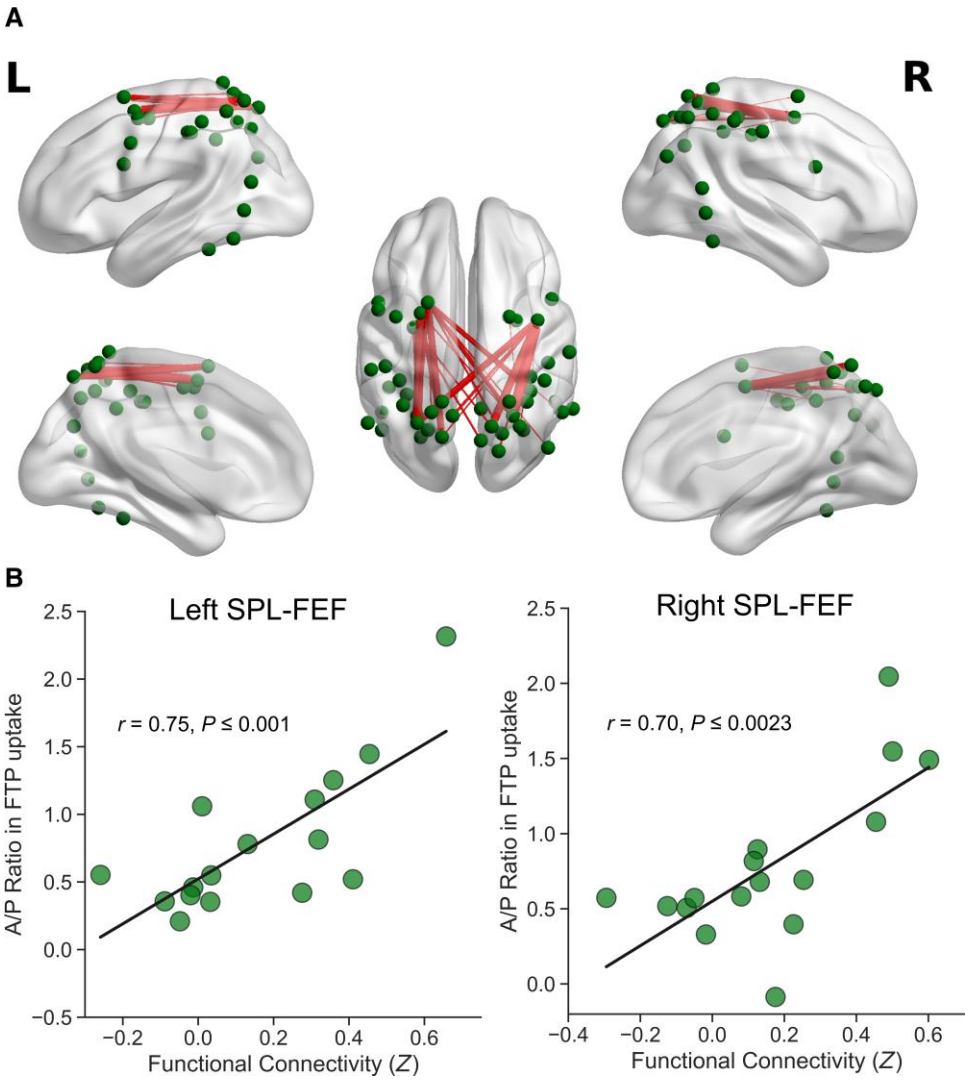

Figure 4 Greater anterior–posterior ratio in FTP uptake is associated with greater intrinsic functional connectivity between the anterior and posterior nodes of the DAN. (**A**) Edges represent pairs of anterior and posterior nodes within the DAN for which intrinsic functional connectivity and the ratio in FTP uptake were positively correlated across patients at $P < 0.05$. Dots identify the location of each node part of the canonical DAN.[38,64] Edge thickness scales with the magnitude of FTP-FC correlation, where thicker edges represent stronger correlations. (**B**) Scatter plots represent significant FTP-FC correlations observed bilaterally between the superior parietal lobule and FEF, two of the key nodes of the DAN.

heterogeneity observed in the pattern of tau accumulation across Alzheimer's disease syndromes, less is known about how tau spreads within specific functional networks in PCA in relation to the hallmark clinical symptoms observed in this syndrome. In this cross-sectional study, we found evidence supporting the hypothesis that tau deposition in PCA starts in the posterior cortical regions within the visual network and DAN, and that visuospatial cognition declines as tau gradually propagates anteriorly within the DAN. These results provide additional support for the network neurodegeneration hypothesis of Alzheimer's disease, suggesting that as key nodes of a given network are affected by tau pathology, cognitive abilities primarily subserved by that network decline.

At the group level, the spatial topography of increased FTP uptake present in our PCA patients relative to control participants was consistent with prior group studies using the same radiotracer, showing prominent localization of cortical tau pathology to the occipital, ventral and lateral temporal, lateral and medial parietal, and lateral frontal cortices.[11,13,14] By employing a well-established functional parcellation of the cerebral cortex, we demonstrated that the visual network and DAN showed the greatest vulnerability to Alzheimer's disease tau pathology. Furthermore, the topography of elevated FTP uptake across patients was remarkably consistent, with 100% of patients showing elevated signal in at least some regions within these two networks. These results are consistent with prior findings demonstrating neurodegenerative disruption of these networks in PCA.[14,23,31] The vulnerability of the visual network and DAN to tau pathology is also in line with the clinical symptoms characteristic of this syndrome, including a progressive impairment in higher-order visuospatial and visuoperceptual processing in the absence of ophthalmological impairment.[2]

Although prior neuroimaging studies of PCA have emphasized structural and functional alterations in posterior cortical regions,[71,72] there is also evidence to suggest that the dysfunction of anterior cortical regions, such as the FEF within the DAN, might be key to characterizing the disease progression of PCA.[23,26,34,73] Supporting this view, we observed that elevated FTP uptake in the anterior DAN (including bilateral FEF) was negatively associated with performance on a measure of visuospatial attention, whereas this relationship was not observed with elevated FTP signal in the posterior DAN (superior parietal lobule and area MT) or the visual network. This is consistent with transcranial magnetic stimulation studies in which modulation of FEF function changed performance on visuospatial attention tasks.[74] This provides additional circumstantial evidence of the spread of tau within the DAN, as neurodegeneration in PCA starts posteriorly and, with the natural progression of disease, spreads to the lateral frontal cortex.[26,73]

The observed pattern of brain–behaviour correlations based on cortical thickness data further underscores the utility of tau pathology in the anterior DAN in predicting cognitive decline in PCA. Atrophy in the posterior cortical regions (visual network and posterior DAN) was more prominent and predictive of deficits in visuospatial attention. In contrast, the degree of atrophy in the anterior DAN was not associated with visual cognitive task performance and did not fundamentally influence the relationship between FTP uptake in this network and visual cognitive deficits. This may be because atrophy within the anterior DAN was not yet detectable at the disease stage of the current sample. These findings are overall consistent with prior studies identifying the effect of tau on cognition independently of cortical atrophy across a syndromic spectrum of Alzheimer's disease including PCA.[14,44] The Tau Network Propagation Index in the DAN, which adjusts the involvement of its anterior nodes for posterior tau pathology in each patient, was most strongly related to visuospatial cognitive deficits compared with measures of anterior or posterior tau alone and those of cortical atrophy in all networks of interest. Taken together, these findings suggest that the Tau Network Propagation Index within the DAN may have utility as a more sensitive biomarker of the molecular pathological correlate of impaired visuospatial attention in PCA. Presumably, interventions limiting the anterior propagation of tau in this network would be expected to improve visuospatial attention in PCA.

Our hypothesis regarding tau propagation in PCA is further substantiated by the result of our cross-modal correlation analysis demonstrating that the magnitude of intrinsic functional connectivity between select pairs of the anterior and posterior nodes of the DAN was directly associated with the level of tau deposition in each of these regions, such that greater intrinsic functional connectivity was related to the Tau Network Propagation Index in the DAN. This suggests that the interregional spread of tau pathology within the DAN might be facilitated by stronger functional connectivity, consistent with prior multimodal neuroimaging studies highlighting the role of connectivity in the spread of tau across Alzheimer's disease syndromic subtypes.[19–22] Furthermore, this finding extends our prior work on the relationship between functional connectivity and neurodegeneration of the temporal pole in semantic variant primary progressive aphasia (svPPA).[75] In that study, we found that the magnitude of atrophy in distributed cortical regions in svPPA patients correlated with the magnitude of functional connectivity between the temporal pole (the presumed origin site of neurodegeneration) and those same distributed cortical regions in healthy individuals. Here, we show that this observation generalizes to functional connectivity data collected from PCA patients and relates to the likely spread of tau pathology within the DAN. We interpret these results as suggesting that individuals who have stronger DAN functional connectivity have a higher Tau Network Propagation Index within the DAN—i.e. stronger network connectivity facilitates spread of tau pathology. It is also possible, however, that tau propagation changes network connectivity leading to an initial increase in connectivity as the circuit becomes dysfunctional.[76] This is an important issue to try to resolve, as it would be possible to use neuromodulation techniques to influence DAN connectivity one way or the other in PCA. Overall, the observed relationship between the Tau Network Propagation Index and intrinsic functional connectivity within the DAN provides insights into possible mechanisms of the disease propagation in PCA, extending prior work emphasizing the deafferentation within the DAN.[26]

The present findings should be interpreted in light of some limitations of the study. First, our relatively small sample size may have rendered some of our analyses (e.g. bivariate correlation) insufficiently powered. It is therefore important for future studies to replicate the observed effects. Second, the cross-sectional nature of this study and its implications for the current findings need to be acknowledged. The results reported here suggest possible mechanisms underlying the propagation of tau within the DAN in PCA over time. However, the spread of tau is only hypothesized here and must therefore be directly tested by examining changes in the distribution and magnitude of tau pathology over time in each patient. Therefore, longitudinal analyses of FTP PET data are required to confirm our interpretations presented here regarding the role of the DAN in the cortical spread of tau in PCA. Third, some of the brain–behaviour relationships were found to be generalizable across several functional networks of the cerebral cortex in our

sample, leaving the specificity of their contributions to cognitive deficits unclear. In the current sample, all of our PCA patients were already symptomatic and FTP uptake was significantly elevated in all cortical functional networks. Relatively greater tau accumulation within the visual network and the DAN may indicate that these networks are preferentially targeted earlier in the disease course. Therefore, dissociable contributions of various networks to deficits in visuospatial attention may be more clearly demonstrated in presymptomatic individuals or those in the earlier stages of symptomatic disease. Finally, due to the limited availability of the data in our sample, we were unable to examine the effect of the ϵ4 allele of APOE (*APOE4*). While the presence of *APOE4* has been shown to interact with the magnitude of cortical FTP uptake in Alzheimer's disease, such an effect appears to be very focal and limited to the medial temporal lobe.[77,78] Therefore, it is unlikely that the present findings are driven by the presence of *APOE4*. Notwithstanding these limitations, the new cross-modal evidence identified here suggests potential mechanisms underlying the spread of tau pathology in PCA by highlighting the role of intrinsic connectivity within the DAN. Future work should further characterize the spatiotemporal pattern of cortical tau spread as it relates to the heterogeneous clinical presentations within the PCA syndrome[2] involving, for instance, individualized prediction of longitudinal tau accumulation patterns on the basis of baseline tau pathology, functional connectivity and prominent symptom characteristics unique to each patient. Such effort would be useful for more accurate characterization of disease progression, which may inform both prognosis as well as potential therapeutic interventions in these patients.

Acknowledgements

The authors would like to thank the patients and families who participated in this research, without whose partnership this research would not have been possible.

Funding

This research was supported by National Institutes of Health grants K23AG065450, K23DC016912, R21AG051987, R01DC014296, P01AG005134 and P30AG062421 and by the David Mooney Family Fund for PCA Research. This research was carried out in part at the Athinoula A. Martinos Center for Biomedical Imaging at the MGH, using resources provided by the Center for Functional Neuroimaging Technologies, P41EB015896, a P41 Biotechnology Resource Grant supported by the National Institute of Biomedical Imaging and Bioengineering (NIBIB), National Institutes of Health. This work also involved the use of instrumentation supported by the NIH Shared Instrumentation Grant Program and/or High-End Instrumentation Grant Program; specifically, grant number(s) S10RR021110, S10RR023043, S10RR023401.

Competing interests

B.C.D. has been a consultant for Acadia, Alector, Arkuda, Biogen, Denali, Lilly, Merck, Novartis, Takeda, Wave Lifesciences, and has received royalties from Cambridge University Press, Elsevier, Oxford University Press.

Supplementary material

Supplementary material is available at *Brain* online.

References

1. Benson DF, Davis RJ, Snyder BD. Posterior cortical atrophy. *Arch Neurol*. 1988;45:789–793.
2. Crutch SJ, Schott JM, Rabinovici GD, *et al*. Consensus classification of posterior cortical atrophy. *Alzheimers Dement*. 2017;13:870–884.
3. Mendez MF, Ghajarania N, Perryman KM. Posterior cortical atrophy: Clinical characteristics and differences compared to Alzheimer's disease. *Dement Geriatr Cogn Disord*. 2002;14:33–40.
4. Renner JA, Burns JM, Hou CE, McKeel DW, Storandt M, Morris JC. Progressive posterior cortical dysfunction. *Neurology*. 2004;63:1175–1180.
5. Tang-Wai DF, Graff-Radford NR, Boeve BF, *et al*. Clinical, genetic, and neuropathologic characteristics of posterior cortical atrophy. *Neurology*. 2004;63:1168–1174.
6. Dickerson BC, McGinnis SM, Xia C, *et al*. Approach to atypical Alzheimer's disease and case studies of the major subtypes. *CNS Spectr*. 2017;22:439–449.
7. Wong B, Lucente DE, MacLean J, *et al*. Diagnostic evaluation and monitoring of patients with posterior cortical atrophy. *Neurodegener Dis Manag*. 2019;9:217–239.
8. Levine DN, Lee JM, Fisher CM. The visual variant of Alzheimer's disease. *Neurology*. 1993;43:305–305.
9. Hof PR. Morphology and neurochemical characteristics of the vulnerable neurons in brain aging and Alzheimer's disease. *Eur Neurol*. 1997;37:71–81.
10. Hof PR, Bouras C, Constandinidis J, Morrison JH. Balit's syndrome in Alzheimer's disease: Specific disruption of the occipito-parietal visual pathway. *Brain Res*. 1989;493:368–375.
11. Day GS, Gordon BA, Jackson K, *et al*. Tau-PET binding distinguishes patients with early-stage posterior cortical atrophy from amnestic Alzheimer disease dementia. *Alzheimer Dis Assoc Disord*. 2017;31:87–93.
12. Ossenkoppele R, Schonhaut DR, Baker SL, *et al*. Tau, amyloid, and hypometabolism in a patient with posterior cortical atrophy. *Ann Neurol*. 2015;77:338–342.
13. Ossenkoppele R, Schonhaut DR, Schöll M, *et al*. Tau PET patterns mirror clinical and neuroanatomical variability in Alzheimer's disease. *Brain*. 2016;139:1551–1567.
14. Putcha D, Brickhouse M, Touroutoglou A, *et al*. Visual cognition in non-amnestic Alzheimer's disease: Relations to tau, amyloid, and cortical atrophy. *Neuroimage Clin*. 2019;23:101889.
15. Xia C, Makaretz SJ, Caso C, *et al*. Association of *in vivo* [18F] AV-1451 tau PET imaging results with cortical atrophy and symptoms in typical and atypical Alzheimer disease. *JAMA Neurol*. 2017;74:427.
16. Xia C, Dickerson BC. Multimodal PET imaging of amyloid and tau pathology in Alzheimer disease and non-Alzheimer disease dementias. *PET Clin*. 2017;12:351–359.
17. Vogel JW, Young AL, Oxtoby NP, *et al*. Four distinct trajectories of tau deposition identified in Alzheimer's disease. *Nat Med*. 2021;27:871–881.
18. Ahmed Z, Cooper J, Murray TK, *et al*. A novel *in vivo* model of tau propagation with rapid and progressive neurofibrillary tangle pathology: The pattern of spread is determined by connectivity, not proximity. *Acta Neuropathol*. 2014;127:667–683.
19. Franzmeier N, Rubinski A, Neitzel J, *et al*. Functional connectivity associated with tau levels in ageing, Alzheimer's, and small vessel disease. *Brain*. 2019;142:1093–1107.

20. Ossenkoppele R, Iaccarino L, Schonhaut DR, *et al*. Tau covariance patterns in Alzheimer's disease patients match intrinsic connectivity networks in the healthy brain. *Neuroimage Clin*. 2019;23:101848.
21. Sintini I, Graff-Radford J, Jones DT, *et al*. Tau and amyloid relationships with resting-state functional connectivity in atypical Alzheimer's disease. *Cereb Cortex*. 2021;31:1693–1706.
22. Franzmeier N, Neitzel J, Rubinski A, *et al*. Functional brain architecture is associated with the rate of tau accumulation in Alzheimer's disease. *Nat Commun*. 2020;11:347.
23. Cerami C, Crespi C, Della Rosa PA, *et al*. Brain changes within the visuo-spatial attentional network in posterior cortical atrophy. *J Alzheimers Dis*. 2015;43:385–395.
24. Lehmann M, Ghosh PM, Madison C, *et al*. Diverging patterns of amyloid deposition and hypometabolism in clinical variants of probable Alzheimer's disease. *Brain*. 2013;136:844–858.
25. Montembeault M, Brambati SM, Gorno-Tempini ML, Migliaccio R. Clinical, anatomical, and pathological features in the three variants of primary progressive aphasia: A review. *Front Neurol*. 2018;9:692.
26. Nestor PJ, Caine D, Fryer TD, Clarke J, Hodges JR. The topography of metabolic deficits in posterior cortical atrophy (the visual variant of Alzheimer's disease) with FDG-PET. *J Neurol Neurosurg Psychiatry*. 2003;74:1521–1529.
27. Migliaccio R, Gallea C, Kas A, *et al*. Functional connectivity of ventral and dorsal visual streams in posterior cortical atrophy. *J Alzheimers Dis*. 2016;51:1119–1130.
28. Agosta F, Mandic-Stojmenovic G, Canu E, *et al*. Functional and structural brain networks in posterior cortical atrophy: a two-centre multiparametric MRI study. *Neuroimage Clin*. 2018;19:901–910.
29. Lehmann M, Madison C, Ghosh PM, *et al*. Loss of functional connectivity is greater outside the default mode network in nonfamilial early-onset Alzheimer's disease variants. *Neurobiol Aging*. 2015;36:2678–2686.
30. Migliaccio R, Agosta F, Basaia S, *et al*. Functional brain connectome in posterior cortical atrophy. *Neuroimage Clin*. 2020;25:102100.
31. Veldsman M, Zamboni G, Butler C, Ahmed S. Attention network dysfunction underlies memory impairment in posterior cortical atrophy. *Neuroimage Clin*. 2019;22:101773.
32. Corbetta M, Patel G, Shulman GL. The reorienting system of the human brain: from environment to theory of mind. *Neuron*. 2008;58:306–324.
33. Fox MD, Snyder AZ, Vincent JL, Corbetta M, Essen DCV, Raichle ME. The human brain is intrinsically organized into dynamic, anticorrelated functional networks. *Proc Natl Acad Sci U S A*. 2005;102:9673–9678.
34. Kas A, de Souza LC, Samri D, *et al*. Neural correlates of cognitive impairment in posterior cortical atrophy. *Brain*. 2011;134:1464–1478.
35. Ahmed S, Loane C, Bartels S, *et al*. Lateral parietal contributions to memory impairment in posterior cortical atrophy. *Neuroimage Clin*. 2018;20:252–259.
36. La Joie R, Visani AV, Baker SL, *et al*. Prospective longitudinal atrophy in Alzheimer's disease correlates with the intensity and topography of baseline tau-PET. *Sci Transl Med*. 2020;12:eaau5732.
37. Sintini I, Graff-Radford J, Senjem ML, *et al*. Longitudinal neuroimaging biomarkers differ across Alzheimer's disease phenotypes. *Brain*. 2020;143:2281–2294.
38. Yeo BTT, Krienen FM, Sepulcre J, *et al*. The organization of the human cerebral cortex estimated by intrinsic functional connectivity. *J Neurophysiol*. 2011;106:1125–1165.
39. Jack CR, Bennett DA, Blennow K, *et al*. A/T/N: An unbiased descriptive classification scheme for Alzheimer disease biomarkers. *Neurology*. 2016;87:539–547.
40. Putcha D, McGinnis SM, Brickhouse M, Wong B, Sherman JC, Dickerson BC. Executive dysfunction contributes to verbal encoding and retrieval deficits in posterior cortical atrophy. *Cortex*. 2018;106:36–46.
41. Rabinovici GD, Furst AJ, Alkalay A, *et al*. Increased metabolic vulnerability in early-onset Alzheimer's disease is not related to amyloid burden. *Brain*. 2010;133:512–528.
42. Villeneuve S, Rabinovici GD, Cohn-Sheehy BI, *et al*. Existing Pittsburgh compound-B positron emission tomography thresholds are too high: Statistical and pathological evaluation. *Brain*. 2015;138:2020–2033.
43. Warrington E, James M. *The visual object and space perception battery*. Thames Valley Test Co; 1991.
44. Bejanin A, Schonhaut DR, La Joie R, *et al*. Tau pathology and neurodegeneration contribute to cognitive impairment in Alzheimer's disease. *Brain*. 2017;140:3286–3300.
45. Shoup TM, Yokell DL, Rice PA, *et al*. A concise radiosynthesis of the tau radiopharmaceutical, [18F]T807. *J Labelled Comp Radiopharm*. 2013;56:736–740.
46. Becker JA, Hedden T, Carmasin J, *et al*. Amyloid-β associated cortical thinning in clinically normal elderly. *Ann Neurol*. 2011;69:1032–1042.
47. Fischl B, Liu A, Dale AM. Automated manifold surgery: Constructing geometrically accurate and topologically correct models of the human cerebral cortex. *IEEE Trans Med Imaging*. 2001;20:70–80.
48. Greve DN, Svarer C, Fisher PM, *et al*. Cortical surface-based analysis reduces bias and variance in kinetic modeling of brain PET data. *Neuroimage*. 2014;92:225–236.
49. Greve DN, Salat DH, Bowen SL, *et al*. Different partial volume correction methods lead to different conclusions: An 18F-FDG-PET study of aging. *Neuroimage*. 2016;132:334–343.
50. Desikan RS, Ségonne F, Fischl B, *et al*. An automated labeling system for subdividing the human cerebral cortex on MRI scans into gyral based regions of interest. *Neuroimage*. 2006;31:968–980.
51. Johnson KA, Schultz A, Betensky RA, *et al*. Tau positron emission tomographic imaging in aging and early Alzheimer disease. *Ann Neurol*. 2016;79:110–119.
52. Putcha D, Eckbo R, Katsumi Y, Dickerson BC, Touroutoglou A, Collins JA. Tau and the fractionated default mode network in atypical Alzheimer's disease. *Brain Commun*. 2022;4:fcac055.
53. La Joie R, Bejanin A, Fagan AM, *et al*. Associations between [18F]AV1451 tau PET and CSF measures of tau pathology in a clinical sample. *Neurology*. 2018;90:e282–e290.
54. Tsai RM, Bejanin A, Lesman-Segev O, *et al*. ^{18}F-flortaucipir (AV-1451) tau PET in frontotemporal dementia syndromes. *Alzheimers Res Ther*. 2019;11:13.
55. La Joie R, Perrotin A, Barré L, *et al*. Region-specific hierarchy between atrophy, hypometabolism, and β-amyloid (aβ) load in Alzheimer's disease dementia. *J Neurosci*. 2012;32:16265–16273.
56. Staffaroni AM, Cobigo Y, Goh SYM, *et al*. Individualized atrophy scores predict dementia onset in familial frontotemporal lobar degeneration. *Alzheimers Dement*. 2020;16:37–48.
57. Biswal B, Zerrin Yetkin F, Haughton VM, Hyde JS. Functional connectivity in the motor cortex of resting human brain using echo-planar MRI. *Magn Reson Med*. 1995;34:537–541.
58. Van Dijk KRA, Hedden T, Venkataraman A, Evans KC, Lazar SW, Buckner RL. Intrinsic functional connectivity as a tool for

human connectomics: Theory, properties, and optimization. *J Neurophysiol*. 2010;103:297–321.
59. Vincent JL, Patel GH, Fox MD, *et al*. Intrinsic functional architecture in the anaesthetized monkey brain. *Nature*. 2007;447:83–86.
60. Popal H, Quimby M, Hochberg D, Dickerson BC, Collins JA. Altered functional connectivity of cortical networks in semantic variant Primary Progressive Aphasia. *Neuroimage Clin*. 2020;28: 102494.
61. Touroutoglou A, Hollenbeck M, Dickerson BC, Barrett LF. Dissociable large-scale networks anchored in the right anterior insula subserve affective experience and attention. *Neuroimage*. 2012;60:1947–1958.
62. Touroutoglou A, Andreano JM, Barrett LF, Dickerson BC. Brain network connectivity–behavioral relationships exhibit trait-like properties: Evidence from hippocampal connectivity and memory. *Hippocampus*. 2015;25:1591–1598.
63. Zhang J, Abiose O, Katsumi Y, Touroutoglou A, Dickerson BC, Barrett LF. Intrinsic functional connectivity is organized as three interdependent gradients. *Sci Rep*. 2019;9:15976.
64. Zhang J, Andreano JM, Dickerson BC, Touroutoglou A, Barrett LF. Stronger functional connectivity in the default mode and salience networks is associated with youthful memory in superaging. *Cereb Cortex*. 2020;30:72–84.
65. Schaefer A, Kong R, Gordon EM, *et al*. Local–global parcellation of the human cerebral cortex from intrinsic functional connectivity MRI. *Cereb Cortex*. 2018;28:3095–3114.
66. Kong R, Li J, Orban C, *et al*. Spatial topography of individual-specific cortical networks predicts human cognition, personality, and emotion. *Cereb Cortex*. 2019;29:2533–2551.
67. Katsumi Y, Theriault JE, Quigley KS, Barrett LF. Allostasis as a core feature of hierarchical gradients in the human brain. PsyArXiv, https://psyarxiv.com/wezv8/, 2021, preprint: not peer reviewed.
68. Kleckner IR, Zhang J, Touroutoglou A, *et al*. Evidence for a large-scale brain system supporting allostasis and interoception in humans. *Nat Hum Behav*. 2017;1:0069.
69. Franzmeier N, Dewenter A, Frontzkowski L, *et al*. Patient-centered connectivity-based prediction of tau pathology spread in Alzheimer's disease. *Sci Adv*. 2020;6:eabd1327.
70. Vogel JW, Iturria-Medina Y, Strandberg OT, *et al*. Spread of pathological tau proteins through communicating neurons in human Alzheimer's disease. *Nat Commun*. 2020;11:2612.
71. Lehmann M, Madison CM, Ghosh PM, *et al*. Intrinsic connectivity networks in healthy subjects explain clinical variability in Alzheimer's disease. *Proc Natl Acad Sci U S A*. 2013;110:11606–11611.
72. Ossenkoppele R, Cohn-Sheehy BI, Joie RL, *et al*. Atrophy patterns in early clinical stages across distinct phenotypes of Alzheimer's disease. *Hum Brain Mapp*. 2015;36:4421–4437.
73. Sintini I, Martin PR, Graff-Radford J, *et al*. Longitudinal tau-PET uptake and atrophy in atypical Alzheimer's disease. *Neuroimage Clin*. 2019;23:101823.
74. Murd C, Moisa M, Grueschow M, Polania R, Ruff CC. Causal contributions of human frontal eye fields to distinct aspects of decision formation. *Sci Rep*. 2020;10:7317.
75. Collins JA, Montal V, Hochberg D, *et al*. Focal temporal pole atrophy and network degeneration in semantic variant primary progressive aphasia. *Brain*. 2017;140:457–471.
76. Das SR, Pluta J, Mancuso L, *et al*. Increased functional connectivity within medial temporal lobe in mild cognitive impairment. *Hippocampus*. 2013;23:1–6.
77. La Joie R, Visani AV, Lesman-Segev OH, *et al*. Association of *APOE4* and clinical variability in Alzheimer disease with the pattern of tau- and amyloid-PET. *Neurology*. 2021;96:e650–e661.
78. Therriault J, Benedet AL, Pascoal TA, *et al*. Association of apolipoprotein E $\epsilon 4$ with medial temporal tau independent of amyloid-β. *JAMA Neurol*. 2020;77:470–479.